

Published in final edited form as:

*Cancer Prev Res (Phila)*. 2014 September ; 7(9): 958–967. doi:10.1158/1940-6207.CAPR-14-0126.

## Kaempferol targets RSK2 and MSK1 to suppress ultraviolet radiation-induced skin cancer

Ke Yao<sup>#1,2</sup>, Hanyong Chen<sup>#1</sup>, Kangdong Liu<sup>#1,2</sup>, Alyssa Langfald<sup>1</sup>, Ge Yang<sup>1,2</sup>, Yi Zhang<sup>1,2</sup>, Dong Hoon Yu<sup>1</sup>, Myoung Ok Kim<sup>1,3</sup>, Mee-Hyun Lee<sup>1,4</sup>, Haitao Li<sup>1</sup>, Ki Beom Bae<sup>1</sup>, Hong-Gyum Kim<sup>1</sup>, Wei-Ya Ma<sup>1</sup>, Ann M. Bode<sup>1</sup>, Ziming Dong<sup>2</sup>, and Zigang Dong<sup>1,\*</sup>

<sup>1</sup> The Hormel Institute, University of Minnesota, 801 16th Ave NE, Austin, MN 55912

<sup>2</sup> Pathophysiology Department, Basic Medical College, Zhengzhou University, No.100 Kexue Road, Henan, China, 450001

# These authors contributed equally to this work.

### Abstract

Solar ultraviolet (SUV) irradiation is a major factor in skin carcinogenesis, the most common form of cancer in the USA. The mitogen-activated protein (MAP) kinase cascades are activated by SUV irradiation. The 90 kDa ribosomal S6 kinase (RSK) and mitogen and stress activated protein kinase (MSK) proteins constitute a family of protein kinases that mediate signal transduction downstream of the MAP kinase cascades. In this study, phosphorylation of RSK and MSK1 was up-regulated in human squamous cell carcinoma (SCC) and solar UV-treated mouse skin. Kaempferol, a natural flavonol, found in tea, broccoli, grapes, apples and other plant sources, is known to have anticancer activity, but its mechanisms and direct target(s) in cancer chemoprevention are unclear. Kinase array results revealed that kaempferol inhibited RSK2 and MSK1. Pull-down assay results, ATP competition and *in vitro* kinase assay data revealed that kaempferol interacts with RSK2 and MSK1 at the ATP-binding pocket and inhibits their respective kinase activities. Mechanistic investigations showed that kaempferol suppresses RSK2 and MSK1 kinase activities to attenuate solar UV-induced phosphorylation of CREB and histone H3 in mouse skin cells. Kaempferol was a potent inhibitor of solar UV-induced mouse skin carcinogenesis. Further analysis showed that skin from the kaempferol-treated group exhibited a substantial reduction in solar UV-induced phosphorylation of cAMP response element-binding protein (CREB), c-Fos and histone H3. Overall, our results identify kaempferol as a safe and novel chemopreventive agent against solar UV-induced skin carcinogenesis that acts by targeting RSK2 and MSK1.

\* **Corresponding Author:** Address correspondence to Zigang Dong; The Hormel Institute University of Minnesota, 801 16th Ave NE, Austin, MN 55912; Telephone: 507-437-9600 FAX: 507-437-9606; zgdong@hi.umn.edu.

<sup>3</sup> Current address: Kyungpook National University, School of Animal BT Science, Center for Laboratory Animal Resources, Daegu, 700-422 South Korea.

<sup>4</sup> Current address: College of Pharmacy, The Catholic University of Korea, 43, Jibong-ro, Wonmi-gu, Bucheon, Gyeonggi-do, Republic of Korea

**Potential Conflicts of Interest:** No potential conflicts of interest

## Keywords

kaempferol; SUV; skin cancer; RSK2; MSK1

---

## Introduction

Over the past three decades, more people have developed skin cancer than all other cancers combined (1). One in five Americans will develop skin cancer in their lifetime (2). Skin cancers are typically diagnosed as basal cell carcinomas (BCC) or squamous cell carcinomas (SCC) (1). Epidemiologic evidence suggests that solar ultraviolet (SUV) irradiation is the most important risk factor for any type of skin cancer (3, 4). SUV comprises approximately 95% UVA and 5% UVB. Both UVA and UVB can cause DNA damage, which is considered a primary etiological factor contributing to the development of skin cancer. Activation of UV-induced cellular signaling pathways plays a vital role in UV-induced skin tumorigenesis. MAP kinases are serine-threonine kinases that control fundamental cellular processes such as growth, proliferation, differentiation, migration and apoptosis. The mammalian MAP kinase family consists of the extracellular signal-regulated kinases (ERKs), c-Jun NH<sub>2</sub>-terminal kinases (JNKs) and p38 (5). Among the MAP kinase family, the ERKs cascade has been a focus of cancer chemoprevention because of its importance in carcinogenesis (6, 7). Abnormalities in the ERKs pathway play a critical role in the development and progression of cancer and its deregulation has been reported in approximately 1/3 of all human cancers (8). The p38 related signal transduction pathway is also markedly affected by SUV exposure (9). The 90 kDa ribosomal S6 kinase (RSK) and mitogen and stress activated protein kinase (MSK) proteins constitute a family of protein kinases that mediate signal transduction downstream of the MAP kinase cascades. RSK is activated by ERKs in response to growth factors, polypeptide hormones, neurotransmitters, chemokines and other stimuli (10). MSK is also activated by ERKs in response to such stimuli, but in addition, MSK can be activated by p38 in response to various cellular stress stimuli and pro-inflammatory cytokines (11). RSK and MSK1 are located between ERKs or p38 and their target transcription factors. We previously reported that RSK2 plays a key role in neoplastic transformation of human skin cells and in skin cancer growth (12, 13). Mice lacking MSK1 show reduced skin tumor development in a two-stage chemical carcinogenesis model (14, 15). Therefore, targeting SUV-induced RSK2 and MSK1 might be an effective strategy for preventing skin tumorigenesis caused by SUV.

Flavonoids are ubiquitously found in fruits and vegetables as well as popular beverages, and reportedly exhibit antioxidant, antitumor, and anti-inflammatory effects (16-18). In particular, their antitumor activity has attracted much attention as a possible dietary prevention strategy against carcinogenesis. Kaempferol, a natural flavonol, isolated from tea, broccoli, grapes, apples and other plant sources, is believed to have anticancer activity, but its molecular mechanisms and direct target(s) in cancer chemoprevention are still unclear. Herein, we report that kaempferol suppresses SUV-induced activation of signal transduction by directly inhibiting RSK2 and MSK1 in mouse skin cells. Moreover, kaempferol strongly suppresses tumor incidence in a SUV-induced skin carcinogenesis

mouse model. Thus, kaempferol acts as an inhibitor of RSK2 and MSK1 and is expected to have beneficial effects in the prevention of SUV-induced skin carcinogenesis.

## Materials and Methods

### Chemicals

Eagle's minimum essential medium (EMEM) and basal medium Eagle (BME) were purchased from Invitrogen (Grand Island, NY). FBS was purchased from Gemini Bio-products (Sacramento, CA). The antibodies against phosphorylated MEK, ERKs, JNKs, p38, RSK, MSK1, CREB, histone H3, and total MEK, ERKs, JNKs, p38, CREB and histone H3 were purchased from Cell Signaling Biotechnology (Danvers, MA). The Ki-67 antibody was purchased from Abcam (Cambridge, MA). Kaempferol and the antibody against  $\beta$ -actin were purchased from Sigma-Aldrich (St. Louis, MO). The Protein Assay Kit was from Bio-Rad (Berkeley, CA), and the CellTiter 96 Aqueous One Solution Cell Proliferation Assay Kit and the luciferase assay substrate were purchased from Promega (Madison, WI). The active RSK2 and MSK1 kinases were obtained from Upstate Biotechnology (Billerica, MA). CNBr-Sepharose 4B and [ $\gamma$ - $^{32}$ P] ATP were purchased from GE Healthcare (Little Chalfont, Buckinghamshire, UK).

### Immunohistochemistry staining

Skin tissues were embedded in paraffin and subjected to immunohistochemistry. Tissues were de-paraffinized and hydrated and then permeabilized with 0.5% Triton X-100/1  $\times$  PBS for 10 min. Tissues were hybridized with p-RSK (1:100), p-MSK1 (1:50) or Ki-67 (1:150) as the primary antibody and biotinylated goat anti-rabbit IgG as the secondary antibody. An ABC kit (Vector Laboratories, Inc., Burlingame, CA) was used to detect protein targets according to the manufacturer's instructions. After developing with 3,3'-diaminobenzidine, the sections were counterstained with hematoxylin and observed by microscope (200X) and analyzed by the Image-Pro Plus software (v. 6.1) (Media Cybernetics, Inc., Bethesda, MD).

### Foci-forming assay

Transformation of NIH3T3 cells was conducted according to standard protocols. Cells were transiently transfected with various combinations of H-Ras<sup>G12V</sup> (50 ng), RSK2 or MSK1 (450 ng), and pcDNA4-mock (compensation for equal amounts of DNA) as indicated in each figure and cells were then cultured in 5% FBS-DMEM for 2 weeks. Foci were fixed with methanol, stained with 0.5% crystal violet and then counted with a microscope and quantified using the Image-Pro PLUS software program.

### Anchorage-independent cell growth assay

Cells ( $8 \times 10^3$ /well) were suspended in 1 mL BME, 10% FBS and 0.33% agar and plated on 3 mL of solidified BME containing 10% FBS and 0.5% agar for 10 days. Colony number was determined by microscope and Image-Pro Plus software (Media Cybernetics, Inc., Bethesda, MD).

### MTS assay

A431, A431 sh-RSK2, A431 sh-MSK1, or A431 sh-RSK2/sh-MSK1 cells were seeded ( $1 \times 10^3$ ) into 96-well plates. After incubation for 24, 48, 72 or 96 h, CellTiter 96® Aqueous One Solution (20  $\mu$ l; Promega) was added and cells incubated for 1 h in a 37°C, 5% CO<sub>2</sub> incubator. Absorbance was read at 492 and 690 nm.

### Kinase assay

Histone H3 was used for an *in vitro* kinase assay with active RSK2 and MSK1. Reactions were performed at 30°C for 30 min in a mixture containing 100 ng active kinase, 2  $\mu$ g histone H3, 50  $\mu$ M unlabeled ATP and 10  $\mu$ M [ $\gamma$ -<sup>32</sup>P] ATP. Reactions were stopped with 6X SDS sample buffer. Samples were boiled, separated by 15% SDS-PAGE, and visualized by autoradiography.

### Pull-down assays

Kaempferol (2.5 mg) was coupled to CNBr-activated Sepharose 4B (GE Healthcare Biosciences, PA) matrix-beads (0.5 g) in 0.5 M NaCl and 40% DMSO (pH 8.3) overnight at 4°C, according to the manufacturer's instructions. Active RSK2 and MSK1 or JB6 P+ cell lysates (500  $\mu$ g) were mixed with kaempferol-conjugated Sepharose 4B beads or with Sepharose 4B beads alone as control (30  $\mu$ L, 50% suspension). Binding was examined by Western blot analysis.

### Molecular modeling

The computer modeling of kaempferol with RSK2 and MSK1 was performed using the Schrödinger Suite 2013 software programs (19). RSK2 and MSK1 crystal structures were prepared under the standard procedures of the Protein Preparation Wizard (Schrödinger Suite 2013). Hydrogen atoms were added consistent with a pH of 7 and all water molecules were removed. The ATP binding site-based receptor grid was generated for docking. Kaempferol was prepared for docking by default parameters using the LigPrep program (Schrödinger). Then, the docking of kaempferol and proteins was accomplished with default parameters under the extra precision (XP) mode using the program Glide. Herein we could get the best-docked representative structures.

### Keratinocyte isolation

Dorsal skin from SKH-1 mice (6-8 weeks old) was harvested and digested with 2.5% trypsin without EDTA for 1.5 h at 32°C. The epidermis was scraped off into 10% FBS-SMEM (Gibco, Grand Island, NY) and stirred at 100 rpm for 20 min at room temperature. The solution was filtered through 70  $\mu$ m Teflon mesh and keratinocytes were centrifuged at 160  $\times$  g for 7 min at 7°C. Cells were plated at a density of  $1 \times 10^6$  cells per 100-mm dish (20).

### Reporter gene assay

Confluent monolayers of JB6 P+ cells stably transfected with an *AP-1* or *NF- $\kappa$ B* luciferase reporter plasmid were trypsinized, and viable cells ( $4 \times 10^4$ ) suspended in 1 mL of 5% FBS-MEM were added to each well of a 24-well plate. Plates were incubated overnight at 37°C in a humidified atmosphere of 5% CO<sub>2</sub>. Cells were incubated in serum-free medium for

another 24 h and then treated for 2 h with kaempferol (0-50  $\mu\text{M}$ ). Cells were then exposed to SUV (60  $\text{kJ}/\text{m}^2$ ) and harvested after 3 h. The cells were finally disrupted with 100  $\mu\text{L}$  of lysis buffer (0.1 mol/L potassium phosphate pH 7.8, 1% Triton X-100, 1 mmol/L dithiothreitol (DTT), and 2 mmol/L EDTA) and luciferase activity was measured using a luminometer (Luminoskan Ascent, Thermo Electro, Waltham, MA).

### Mouse skin tumorigenesis study

Female SKH-1 hairless mice were purchased from Charles River and maintained under "specific pathogen-free" conditions according to guidelines established by Research Animal Resources, University of Minnesota. The skin carcinogenesis experiments were conducted using mice of 6 to 8 weeks of age with a mean body weight of 25 g. Skin carcinogenesis in mice was induced using a SUV irradiation system. The SUV irradiation source (Q-Lab Corporation, Westlake, OH) emitted at wavelengths of 295 to 365 nm and the peak emission was 340 nm. SKH-1 mice were divided into 5 groups of 12 or 24 animals each. In the control group, the dorsal skin was topically treated with 150  $\mu\text{L}$  of acetone or 1.0 mg kaempferol in 150  $\mu\text{L}$  of acetone only. In the SUV treated group, the dorsal skin was topically treated with 150  $\mu\text{L}$  of acetone 1 h before exposure to SUV. The mice in groups 3 and 4 received topical application of kaempferol (0.5 or 1 mg, respectively) in 150  $\mu\text{L}$  of acetone 1 h before SUV irradiation. At week 1, the SUV dose was 30  $\text{kJ}/\text{m}^2$  UVA and 1.8  $\text{kJ}/\text{m}^2$  UVB, 3 times per week. The dose of SUV was progressively increased (10% each week). At week 6, the dose was 48  $\text{kJ}/\text{m}^2$  UVA and 2.9  $\text{kJ}/\text{m}^2$  UVB and this dose was maintained for weeks 6 to 12. Tumor number and volume were recorded every week until the end of the experiment. One-half of the samples were immediately fixed in 10% formalin and processed for hematoxylin and eosin (H&E) staining and immunohistochemistry. The other samples were frozen and used for Western blot analysis.

### Statistical analysis

All quantitative data are expressed as mean values  $\pm$  S.D. or  $\pm$  S.E. and significant differences were determined by Student t test or one-way ANOVA. A  $p$  value of  $< 0.05$  was used as the criterion for statistical significance.

## Results

### Phosphorylated RSK and MSK1 are highly expressed in SUV-exposed mouse skin and human SCCs

SUV light can be very harmful to human health, causing inflammation, erythema, sunburn, photoaging, and skin cancer (21). The MAP kinases, including ERKs, JNKs and p38, are involved in UV light-induced inflammation and related signal transduction (6). However, the primary signal transduction pathway(s) and key molecules involved in SUV-induced tumorigenesis are not yet completely elucidated. We previously reported that the ERKs and p38 signaling cascades are markedly activated by SUV and play important roles in SUV-induced skin carcinogenesis (8, 9). We found that the phosphorylation levels of the MEK and ERKs cascade were increased in a time- and dose-dependent manner by SUV, with the peak phosphorylation level occurring at 15 min after SUV (60  $\text{kJ}/\text{m}^2$ ) exposure (Fig. S1A, B). We also reported that RSK2 and MSK1 are key regulators in tumor promoter-induced

cell transformation (11, 22). RSK2 and MSK1 are direct substrate kinases of ERKs or p38 and might be required for SUV-induced skin carcinogenesis. In order to confirm our hypothesis, we examined the level of phosphorylated RSK2 or MSK1 in SKH-1 mouse skin exposed to SUV for 12 weeks compared with normal unexposed skin. We observed that chronic SUV exposure dramatically induced RSK and MSK1 phosphorylation (Fig. 1A, B). To further investigate the function of RSK2 and MSK1 in SUV-induced skin cancer, we examined the level of phosphorylated RSK2 and MSK1 in human squamous cell carcinoma (SCC) samples compared with normal skin. Our data indicated that phosphorylated RSK and MSK1 are significantly increased in SCCs (Fig. 1C, D). This suggests that the RSK and MSK1 cascades could play an important role in SUV-induced skin cancer.

### **RSK2 and MSK1 play an important role in anchorage-independent skin cancer cell growth and proliferation**

SUV irradiation rapidly activates the epidermal growth factor receptor (EGFR) through the induction of EGFR ligands and the inactivation of cytoplasmic protein tyrosine phosphatases (23). EGFR is activated by UV radiation and is overexpressed in UV-induced human skin cancers (24). A431 cells comprise an EGFR-amplified human squamous carcinoma cell line. After knocking down expression of RSK2 or MSK1, A431 anchorage-independent cell growth was inhibited. Moreover, colony formation was more substantially decreased in double knock down RSK2 and MSK1 cells (Fig. 2A). Similar effects were observed in proliferation of A431 cells transfected with mock, sh-RSK2, sh-MSK1 or sh-RSK2/sh-MSK1 (Fig. 2B). Double knock down of RSK2 and MSK1 showed the most significant inhibitory effect. Mutations in *ras*, particularly *H-Ras*, are frequent in SCCs (25, 26). To further examine the role of endogenous RSK2 and MSK1 signaling in Ras-induced cell transformation, we conducted a Ras<sup>G12V</sup>-mediated foci-formation assay in NIH3T3 cells. We introduced various combinations of Ras<sup>G12V</sup>, RSK2 and MSK1 into NIH3T3 cells and foci formation was measured. The results indicated that Ras<sup>G12V</sup> induced foci formation and Ras<sup>G12V</sup>/RSK2 or Ras<sup>G12V</sup>/MSK1 substantially enhanced foci formation (Fig. S2). Further, the number of foci induced by the introduction of Ras<sup>G12V</sup>/RSK2 or Ras<sup>G12V</sup>/MSK1 was increased more with co-introduction of Ras<sup>G12V</sup>/RSK2/MSK1. However size was not affected. These results indicate that RSK2 and MSK1 are potential targets for prevention of SUV-induced skin cancer.

### **Kaempferol inhibits RSK2 and MSK1 activity by competing with ATP for binding**

Flavonoids found in many foods exhibit antioxidant, antitumor, and anti-inflammatory effects (27). We previously demonstrated that kaempferol, a flavonol, is a natural compound that inhibits RSK2 kinase activity and attenuates JB6 P+ cell transformation induced by EGF. To determine potential targets of kaempferol, kinase assays were conducted by Millipore's Kinase Profiler Service according to their established protocols. Scores represent the percent of control, which was derived from the following formula: % of control = [(sample – mean no enzyme) / (mean plus enzyme – mean no enzyme)] × 100. The results revealed that RSK2 and MSK1 were the most relevant potential targets of kaempferol compared with other members of the MAP kinase family (Fig. S3A). To further confirm this finding, we conducted an *in vitro* kinase assay with active RSK2 and histone H3 as substrate with ATP. RSK2 activity was strongly suppressed by kaempferol (Fig. 3A). As expected,

kaempferol also had a similar effect on MSK1 activity (Fig. 3B). These results indicate that kaempferol might be a dual inhibitor of both RSK2 and MSK1. To further examine this idea, we conjugated kaempferol with CNBr-Sepharose 4B beads and conducted a pull-down assay. We confirmed that active RSK2 (100 ng) binds with kaempferol-Sepharose 4B beads, but not with Sepharose 4B beads alone (Fig. 3C, upper panel). Using JB6 P+ mouse epidermal cell lysates, we performed another pull-down assay and results revealed that kaempferol also binds with RSK2 in JB6 P+ mouse epidermal cells (Fig. 3C, middle panel). Results of an ATP competition assay showed that the binding ability of kaempferol with RSK2 (Fig. 3C, lower panel) was altered in the presence of ATP. Similar results were obtained for MSK1 in vitro (Fig. 3D, upper panel) and in cells (Fig. 3D, middle panel).

Also, kaempferol bound with MSK1 competitive with ATP (Fig. 3D, lower panel). These data were supported by our computer modeling results (Fig. S3B, C). We also observed that kaempferol does not bind with JNK2 or p38 in JB6 P+ cells (Fig. S3D). All these data confirmed our hypothesis that kaempferol binds and inhibits RSK2 or MSK1 activity in an ATP-competitive manner.

### **Kaempferol attenuates SUV-induced phosphorylation of CREB and histone H3 in mouse skin cells**

RSK2 and MSK1 are activated by growth factors, peptide hormones, or SUV. Numerous proteins, such as the cAMP response element-binding protein (CREB), histones, activating transcription factor 1 (ATF1) and transcription factor activator protein-1 (AP-1), are phosphorylated by active RSK2 and MSK1 (28-30). To examine the effect of kaempferol on SUV-induced skin carcinogenesis, we first determined the effect of kaempferol on MAP kinase signaling in JB6 P+ mouse epidermal skin cells. Results indicated that SUV (6 kJ/m<sup>2</sup>) substantially induced phosphorylation of MEK, ERKs, RSK and MSK1 in JB6 P+ cells harvested at 15 min after SUV. However, phosphorylation of these kinases was not changed by increasing doses of kaempferol (Fig. 4A, left panel). On the other hand, the phosphorylation of CREB, ATF1 and histone H3, which are well known substrates of RSK2 and MSK1, was suppressed by kaempferol in dose-dependent manner (Fig. 4A, right panel). To further confirm our findings, we performed the same experiment in primary keratinocytes isolated from SKH-1 mice. Similarly, phosphorylation of CREB, ATF1 and histone H3 was attenuated by kaempferol (Fig. 4B, right panel), whereas phosphorylation of MEK, ERKs, RSK and MSK1 was not affected (Fig. 4B, left panel). AP-1 and nuclear factor kappa B (NF- $\kappa$ B) are activated through the MAP kinase pathways upon stimulation with UV (31, 32). RSK2 and MSK1 are known to transmit signals downstream to regulate the transcriptional activity of proteins such as AP-1 and NF- $\kappa$ B (33). To examine the effect of kaempferol on SUV-induced transactivation of AP-1 and NF- $\kappa$ B, we exposed JB6 P+ cells stably transfected with an *AP-1* or *NF- $\kappa$ B* luciferase reporter plasmid to kaempferol and SUV. Results indicated that kaempferol suppressed SUV-induced transactivation of AP-1 (Fig. 4C, left) and NF- $\kappa$ B (Fig. 4C, right) in a dose-dependent manner. Based on these results, we hypothesized that kaempferol might effectively reduce SUV-induced carcinogenesis *in vivo*.

## Kaempferol significantly suppresses SUV-induced skin carcinogenesis in a mouse skin tumorigenesis model

To study the anti-tumorigenic activity of kaempferol *in vivo*, we evaluated the effect of kaempferol in a SUV-induced mouse skin tumorigenesis model. SUV irradiation consists of UVA and UVB and thus, more closely resembles the natural environment. Topical application of kaempferol on mouse skin resulted in a substantial inhibition of SUV-induced tumor incidence (Fig. 5A) and also decreased the average tumor volume per mouse (Fig. 5B). At 25 weeks after SUV exposure, results showed that topical treatment with 0.5 or 1 mg kaempferol reduced tumor volume by 56% or 68%, respectively, compared with the vehicle-treated group. Furthermore, treatment with 0.5 or 1 mg kaempferol also reduced tumor incidence by 78% or 91%, respectively, compared with the vehicle-treated group. Skin and tumor samples were processed for H&E staining at the end of the study (25 weeks). Epidermal thickness, caused by edema and epithelial cell proliferation, represents typical skin histological inflammatory alterations (34). UV-induced skin inflammation is usually quantified by measurement of the epidermal thickness (35). The protective effect of compounds against UV-induced skin inflammation is confirmed by the observation of decreases in epidermal thickness (35-37). After treatment with solar UV, epidermal thickness was increased in the vehicle/SUV-treated group. Notably, kaempferol significantly decreased epidermal thickness (Fig. 5C upper panels). Immunohistochemical data showed that Ki-67, which is a well-known cellular marker for proliferation, dramatically increased in the vehicle/SUV-treated group compared with the vehicle group. However, in the kaempferol-treated groups, Ki-67 expression was decreased compared with the vehicle/SUV-treated group (Fig. 5C, lower panels). Western blot analysis of the mouse skin showed that phosphorylation of CREB, c-Fos and histone H3 induced by SUV were dramatically suppressed in the kaempferol-treated group (Fig. 5D). These results clearly showed that kaempferol exerts a strong preventive effect against SUV-induced mouse skin carcinogenesis by inhibiting the activation of RSK2 and MSK1.

## Discussion

UV light is a well-known environmental carcinogen and is highly associated with skin carcinogenesis (38, 39). Squamous cell carcinomas (SCCs) of the skin occur predominantly on UV-exposed areas of the body and have been linked with chronic exposure to UV (40). Studies in various skin cell lines have demonstrated that EGFR and MAP kinases are specific signaling molecules in UV-induced skin carcinogenesis (41, 42). SUV treatment markedly enhances ERKs and p38 signaling, and inhibition of ERKs or p38 results in fewer and smaller tumors in mice exposed to chronic SUV (8, 9). The ERKs/RSK2 pathway regulates cell proliferation, survival, growth, motility and tumorigenesis (22). ERKs are important in regulating cellular functions and double knockout of ERK1 and ERK2, results in mortality of newborn pups within 1 day (43). MSK1 is activated in response to EGF, TPA and UV stimuli (44, 45). RSK2 and MSK1 act downstream of ERKs and p38 and are located between ERKs and its own target transcription factors, including CREB, ATF1 and histone H3. In mouse epithelial cells and keratinocytes exposed to SUV, MAP kinase signaling cascades and downstream transcription factors such as CREB, ATF1 and histone H3 are activated (Fig. 4A, B). Chronic SUV exposure markedly induced phosphorylation of RSK



and MSK1 in human SCCs (Fig. 1C, D). Mouse skin exposed to long term SUV also express high levels of phosphorylated RSK and MSK1 (Fig. 1A, B). In an NIH3T3 cell foci formation assay, the number of foci was increased more by co-introduction of Ras<sup>G12V</sup>/RSK2/MSK1 (Fig. S2). After knocking down RSK2 and MSK1 expression, human A431 skin cancer cell colony formation and growth were significantly inhibited (Fig. 2A, B). These data indicate that targeting RSK2 and MSK1 might be sufficient to prevent skin cancer and also might avoid unwanted side effects associated with targeting upstream kinases (43, 46). Many anticancer drugs exert adverse side effects, which can be severe and life-threatening. Thus, identification of novel anticancer compounds from natural products might be a safer alternative and a promising strategy for cancer prevention or treatment (47). Epidemiological studies indicated that high dietary intake of flavonoids found in fruits and vegetables is associated with a lower cancer incidence (48). Kaempferol is present in a wide variety of fruits and vegetables. In a previous study, we showed that kaempferol inhibited EGF-induced cell transformation (22). However, data showing that kaempferol could act as a cancer prevention agent *in vivo* was still not available. In the present study, kaempferol markedly suppressed SUV-induced skin carcinogenesis in a mouse skin tumorigenesis model by targeting RSK2 and MSK1 (Fig. 3A, B; Fig. 5A, B). The data showed that topical application of kaempferol (1 mg) markedly delayed tumor growth until 21 (measureable size) weeks compared with vehicle control, which was first observable at 13 weeks (Fig. 5A). By the end of the study (25 weeks), 1 mg kaempferol significantly reduced tumor volume and incidence by 68% and 91% compared with the vehicle control.

Overall, our results showed that kaempferol exerted excellent inhibitory effects against UV-induced skin carcinogenesis by directly targeting RSK2 and MSK1. Thus, kaempferol could have highly beneficial effects in the prevention of skin carcinogenesis.

## Supplementary Material

Refer to Web version on PubMed Central for supplementary material.

## Acknowledgments

We thank the University of Arizona Cancer Center for providing the human AK and normal skin tissue samples. We thank Dr. Dong Joon Kim, Sung Keun Jung and Todd Schuster for supporting experiments and Nicki Brickman for assistance in submitting our manuscript (The Hormel Institute, University of Minnesota).

Financial Support:

This work was supported by National Institutes of Health grants: CA166011 (Z. Dong), CA172457 (Z. Dong), CA027502 (Z. Dong), and ES016548 (Z. Dong). The Hormel Foundation and Mayo Foundation, the University of Minnesota and National Natural Science Foundation of China, NSFC Number: 81000926 (Z. Dong).

## References

1. Stern RS. Prevalence of a history of skin cancer in 2007: results of an incidence-based model. *Arch Dermatol.* 2010; 146:279–82. [PubMed: 20231498]
2. Robinson JK. Sun exposure, sun protection, and vitamin D. *JAMA.* 2005; 294:1541–3. [PubMed: 16193624]
3. Berwick M, Lachiewicz A, Pestak C, Thomas N. Solar UV exposure and mortality from skin tumors. *Adv Exp Med Biol.* 2008; 624:117–24. [PubMed: 18348452]

4. de Gruij FR. Skin cancer and solar UV radiation. *Eur J Cancer*. 1999; 35:2003–9. [PubMed: 10711242]
5. Chang L, Karin M. Mammalian MAP kinase signalling cascades. *Nature*. 2001; 410:37–40. [PubMed: 11242034]
6. Bode AM, Dong Z. Mitogen-activated protein kinase activation in UV-induced signal transduction. *Sci STKE*. 2003; 2003:RE2. [PubMed: 12554854]
7. Dhillon AS, Hagan S, Rath O, Kolch W. MAP kinase signalling pathways in cancer. *Oncogene*. 2007; 26:3279–90. [PubMed: 17496922]
8. Li J, Malakhova M, Mottamal M, Reddy K, Kurinov I, Carper A, et al. Norathyriol suppresses skin cancers induced by solar ultraviolet radiation by targeting ERK kinases. *Cancer Res*. 2012; 72:260–70. [PubMed: 22084399]
9. Liu K, Yu D, Cho YY, Bode AM, Ma W, Yao K, et al. Sunlight UV-induced skin cancer relies upon activation of the p38alpha signaling pathway. *Cancer Res*. 2013; 73:2181–8. [PubMed: 23382047]
10. Frodin M, Jensen CJ, Merienne K, Gammeltoft S. A phosphoserine-regulated docking site in the protein kinase RSK2 that recruits and activates PDK1. *EMBO J*. 2000; 19:2924–34. [PubMed: 10856237]
11. Kim HG, Lee KW, Cho YY, Kang NJ, Oh SM, Bode AM, et al. Mitogen- and stress-activated kinase 1-mediated histone H3 phosphorylation is crucial for cell transformation. *Cancer Res*. 2008; 68:2538–47. [PubMed: 18381464]
12. Cho YY, Yao K, Pugliese A, Malakhova ML, Bode AM, Dong Z. A regulatory mechanism for RSK2 NH(2)-terminal kinase activity. *Cancer Res*. 2009; 69:4398–406. [PubMed: 19435896]
13. Cho YY, Lee MH, Lee CJ, Yao K, Lee HS, Bode AM, et al. RSK2 as a key regulator in human skin cancer. *Carcinogenesis*. 2012; 33:2529–37. [PubMed: 22918890]
14. Chang S, Iversen L, Kragballe K, Arthur JS, Johansen C. Mice lacking MSK1 and MSK2 show reduced skin tumor development in a two-stage chemical carcinogenesis model. *Cancer Invest*. 2011; 29:240–5. [PubMed: 21314333]
15. Liu H, Hwang J, Li W, Choi TW, Liu K, Huang Z, et al. A derivative of chrysin suppresses two-stage skin carcinogenesis by inhibiting mitogen- and stress-activated kinase 1. *Cancer Prev Res (Phila)*. 2014; 7:74–85. [PubMed: 24169959]
16. Li ZD, Hu XW, Wang YT, Fang J. Apigenin inhibits proliferation of ovarian cancer A2780 cells through Id1. *FEBS Lett*. 2009; 583:1999–2003. [PubMed: 19447105]
17. Zhou Q, Yan B, Hu X, Li XB, Zhang J, Fang J. Luteolin inhibits invasion of prostate cancer PC3 cells through E-cadherin. *Mol Cancer Ther*. 2009; 8:1684–91. [PubMed: 19509250]
18. Byun S, Lee KW, Jung SK, Lee EJ, Hwang MK, Lim SH, et al. Luteolin inhibits protein kinase C(epsilon) and c-Src activities and UVB-induced skin cancer. *Cancer Res*. 2010; 70:2415–23. [PubMed: 20215519]
19. Schrödinger. Schrödinger Suite 2013. Schrödinger, LLC; New York, NY: 2013. 2013
20. Trempus CS, Morris RJ, Bortner CD, Cotsarelis G, Faircloth RS, Reece JM, et al. Enrichment for living murine keratinocytes from the hair follicle bulge with the cell surface marker CD34. *J Invest Dermatol*. 2003; 120:501–11. [PubMed: 12648211]
21. Zaidi MR, De Fabo EC, Noonan FP, Merlino G. Shedding light on melanocyte pathobiology in vivo. *Cancer Res*. 2012; 72:1591–5. [PubMed: 22422936]
22. Cho YY, Yao K, Kim HG, Kang BS, Zheng D, Bode AM, et al. Ribosomal S6 kinase 2 is a key regulator in tumor promoter induced cell transformation. *Cancer Res*. 2007; 67:8104–12. [PubMed: 17804722]
23. Scaltriti M, Baselga J. The epidermal growth factor receptor pathway: a model for targeted therapy. *Clin Cancer Res*. 2006; 12:5268–72. [PubMed: 17000658]
24. Oi N, Chen H, Ok Kim M, Lubet RA, Bode AM, Dong Z. Taxifolin suppresses UV-induced skin carcinogenesis by targeting EGFR and PI3K. *Cancer Prev Res (Phila)*. 2012; 5:1103–14. [PubMed: 22805054]
25. Geryk-Hall M, Yang Y, Hughes DP. Driven to death: inhibition of farnesylation increases Ras activity in osteosarcoma and promotes growth arrest and cell death. *Mol Cancer Ther*. 2010; 9:1111–9. [PubMed: 20406948]

26. Tsao H, Chin L, Garraway LA, Fisher DE. Melanoma: from mutations to medicine. *Genes Dev.* 2012; 26:1131–55. [PubMed: 22661227]
27. Katiyar SK, Athar M. Grape seeds: ripe for cancer chemoprevention. *Cancer Prev Res (Phila).* 2013; 6:617–21. [PubMed: 23771521]
28. Liu K, Cho YY, Yao K, Nadas J, Kim DJ, Cho EJ, et al. Eriodictyol inhibits RSK2-ATF1 signaling and suppresses EGF-induced neoplastic cell transformation. *J Biol Chem.* 2011; 286:2057–66. [PubMed: 21098035]
29. Keum YS, Kim HG, Bode AM, Surh YJ, Dong Z. UVB-induced COX-2 expression requires histone H3 phosphorylation at Ser10 and Ser28. *Oncogene.* 2013; 32:444–52. [PubMed: 22391560]
30. Cho YY, He Z, Zhang Y, Choi HS, Zhu F, Choi BY, et al. The p53 protein is a novel substrate of ribosomal S6 kinase 2 and a critical intermediary for ribosomal S6 kinase 2 and histone H3 interaction. *Cancer Res.* 2005; 65:3596–603. [PubMed: 15867353]
31. Huang C, Ma WY, Dong Z. The extracellular-signal-regulated protein kinases (Erks) are required for UV-induced AP-1 activation in JB6 cells. *Oncogene.* 1999; 18:2828–35. [PubMed: 10362253]
32. Wang J, Ouyang W, Li J, Wei L, Ma Q, Zhang Z, et al. Loss of tumor suppressor p53 decreases PTEN expression and enhances signaling pathways leading to activation of activator protein 1 and nuclear factor kappaB induced by UV radiation. *Cancer Res.* 2005; 65:6601–11. [PubMed: 16061640]
33. Peng C, Cho YY, Zhu F, Xu YM, Wen W, Ma WY, et al. RSK2 mediates NF- $\kappa$ B activity through the phosphorylation of IkappaB $\alpha$  in the TNF-R1 pathway. *FASEB J.* 2010; 24:3490–9. [PubMed: 20385620]
34. Gambichler T, Boms S, Stucker M, Moussa G, Kreuter A, Sand M, et al. Acute skin alterations following ultraviolet radiation investigated by optical coherence tomography and histology. *Arch Dermatol Res.* 2005; 297:218–25. [PubMed: 16215762]
35. Cole N, Sou PW, Ngo A, Tsang KH, Severino JA, Arun SJ, et al. Topical ‘Sydney’ propolis protects against UV-radiation-induced inflammation, lipid peroxidation and immune suppression in mouse skin. *Int Arch Allergy Immunol.* 2010; 152:87–97. [PubMed: 20016191]
36. Vicentini FT, Fonseca YM, Pitol DL, Iyomasa MM, Bentley MV, Fonseca MJ. Evaluation of protective effect of a water-in-oil microemulsion incorporating quercetin against UVB-induced damage in hairless mice skin. *J Pharm Pharm Sci.* 2010; 13:274–85. [PubMed: 20816012]
37. Jin XJ, Kim EJ, Oh IK, Kim YK, Park CH, Chung JH. Prevention of UV-induced skin damages by 11,14,17-eicosatrienoic acid in hairless mice in vivo. *J Korean Med Sci.* 2010; 25:930–7. [PubMed: 20514317]
38. Bowden GT. Prevention of non-melanoma skin cancer by targeting ultraviolet-B-light signalling. *Nat Rev Cancer.* 2004; 4:23–35. [PubMed: 14681688]
39. Leiter U, Garbe C. Epidemiology of melanoma and nonmelanoma skin cancer--the role of sunlight. *Adv Exp Med Biol.* 2008; 624:89–103. [PubMed: 18348450]
40. Filipowicz E, Adegboyega P, Sanchez RL, Gatalica Z. Expression of CD95 (Fas) in sun-exposed human skin and cutaneous carcinomas. *Cancer.* 2002; 94:814–9. [PubMed: 11857317]
41. Zhang Y, Dong Z, Bode AM, Ma WY, Chen N. Induction of EGFR-dependent and EGFR-independent signaling pathways by ultraviolet A irradiation. *DNA Cell Biol.* 2001; 20:769–79. [PubMed: 11879570]
42. Chen W, Tang Q, Gonzales MS, Bowden GT. Role of p38 MAP kinases and ERK in mediating ultraviolet-B induced cyclooxygenase-2 gene expression in human keratinocytes. *Oncogene.* 2001; 20:3921–6. [PubMed: 11439356]
43. Satoh Y, Kobayashi Y, Takeuchi A, Pages G, Pouyssegur J, Kazama T. Deletion of ERK1 and ERK2 in the CNS causes cortical abnormalities and neonatal lethality: Erk1 deficiency enhances the impairment of neurogenesis in Erk2-deficient mice. *J Neurosci.* 2011; 31:1149–55. [PubMed: 21248139]
44. Park J, Al-Ramahi I, Tan Q, Mollema N, Diaz-Garcia JR, Gallego-Flores T, et al. RAS-MAPK-MSK1 pathway modulates ataxin 1 protein levels and toxicity in SCA1. *Nature.* 2013; 498:325–31. [PubMed: 23719381]

45. Lee CC, Lin YH, Chang WH, Lin PC, Wu YC, Chang JG. Squamocin modulates histone H3 phosphorylation levels and induces G1 phase arrest and apoptosis in cancer cells. *BMC Cancer*. 2011; 11:58. [PubMed: 21299907]
46. Sweeney SE, Firestein GS. Mitogen activated protein kinase inhibitors: where are we now and where are we going? *Ann Rheum Dis*. 2006; 65(Suppl 3):iii83–8. [PubMed: 17038480]
47. Saud SM, Young MR, Jones-Hall YL, Ileva L, Egbuomwan MO, Wise J, et al. Chemopreventive activity of plant flavonoid isorhamnetin in colorectal cancer is mediated by oncogenic Src and beta-catenin. *Cancer Res*. 2013; 73:5473–84. [PubMed: 23824743]
48. Ren W, Qiao Z, Wang H, Zhu L, Zhang L. Flavonoids: promising anticancer agents. *Med Res Rev*. 2003; 23:519–34. [PubMed: 12710022]

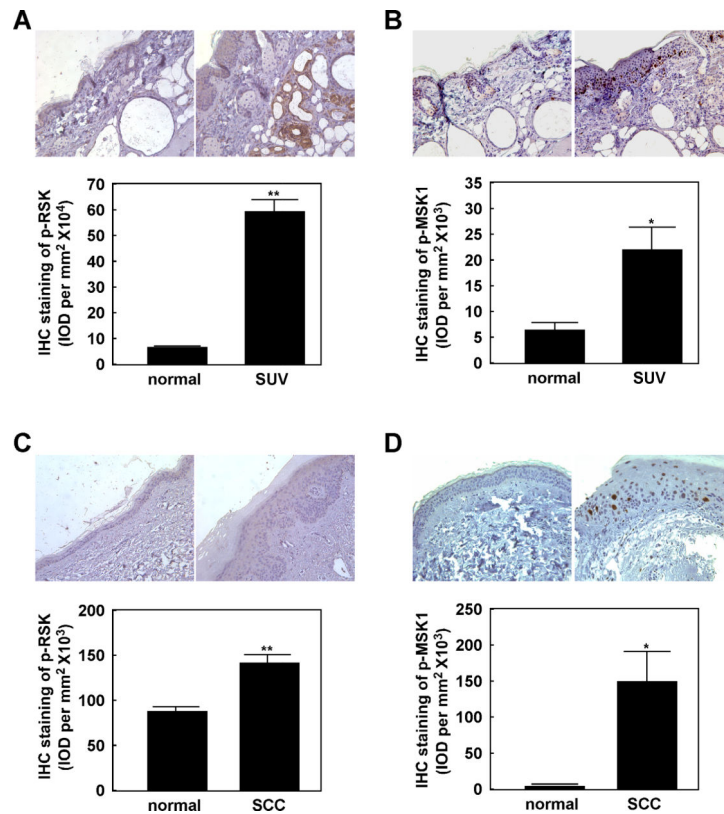


**Figure 1. Phosphorylated RSK (p-RSK) and phosphorylated MSK1 (p-MSK1) are highly expressed in SUV-exposed mouse skin and human SCCs**

Immunohistochemical analysis of p-RSK (A) and p-MSK1 (B) in normal mouse skin and SUV-treated mouse skin samples. Immunohistochemical analysis of p-RSK (C) and p-MSK1 (D) in normal human skin and human SCC samples. Tissue slides from each group were prepared in paraffin sections after fixation with formalin and then stained with the indicated antibodies. Expression of p-RSK or p-MSK1 was visualized by microscopy. Stained cells were counted from 5 separate areas on each slide and an average of 3 samples was calculated per group. Data are expressed as mean percent of control  $\pm$  S.D. The asterisk indicates a significant increase in p-RSK or p-MSK1 expression (\*,  $p < 0.05$ ; \*\*,  $p < 0.01$ ).

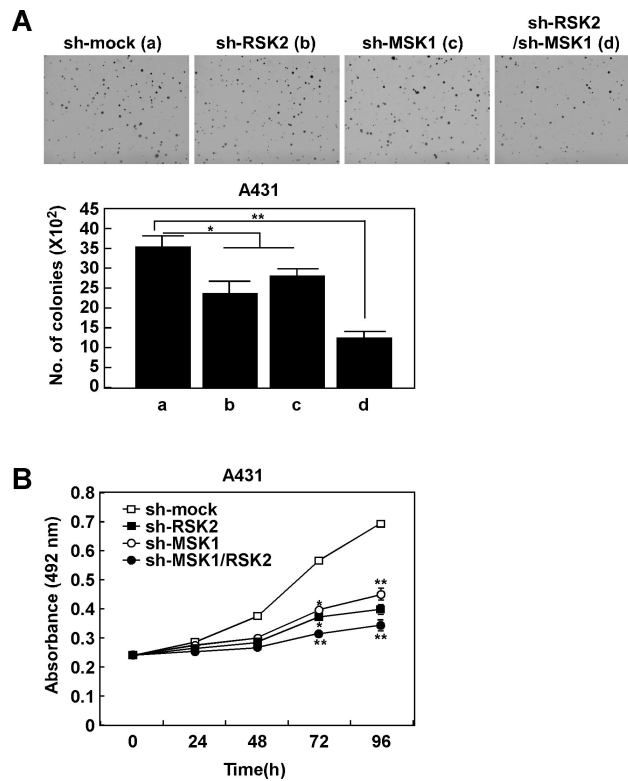


**Figure 2. RSK2 and MSK1 play an important role in anchorage-independent and-dependent skin cancer cell growth**

Knocking down RSK2 or MSK1 expression inhibits A431 anchorage-independent cell growth and proliferation. A431 cells stably expressing sh-mock, sh-RSK2, sh-MSK1 or sh-RSK2/sh-MSK1 were evaluated for colony growth under anchorage-independent conditions (A). Proliferation of A431 cells stably expressing sh-mock, sh-RSK2, sh-MSK1 or sh-RSK2/sh-MSK1 was measured by MTS assay at the indicated time point (B). Data are shown as mean values  $\pm$  S.D. obtained from triplicate experiments. Significant differences were evaluated using one-way ANOVA and the asterisks indicate a significant effect (\*,  $p < 0.05$ ; \*\*,  $p < 0.01$ ).

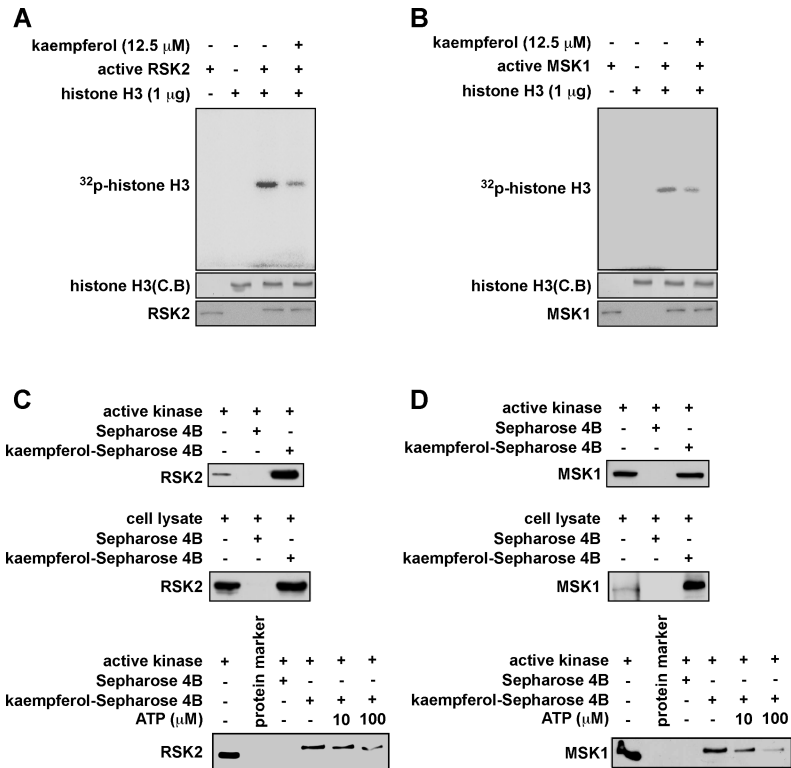


**Figure 3. Kaempferol inhibits RSK2 and MSK1 activity by competing with ATP**

(A-B) Individual *in vitro* kinase assays were conducted using 1  $\mu$ g of histone H3 bacterial-expressed protein, [ $\gamma$ - $^{32}$ P] ATP, kaempferol (12.5  $\mu$ M), and 100 ng of each active RSK2 or MSK1 protein.  $^{32}$ P-labeled phosphorylated histone H3 was visualized by autoradiography. Kaempferol binds with RSK2 (C) and MSK1 (D) in an ATP-competitive manner. Active RSK2 or MSK1 or whole lysates from JB6 P+ cells were incubated with 30  $\mu$ L of kaempferol-Sepharose 4B beads (50% slurry) for 2 h at 4 $^{\circ}$ C. Beads were washed and RSK2 or MSK1 binding was visualized by Western blotting.

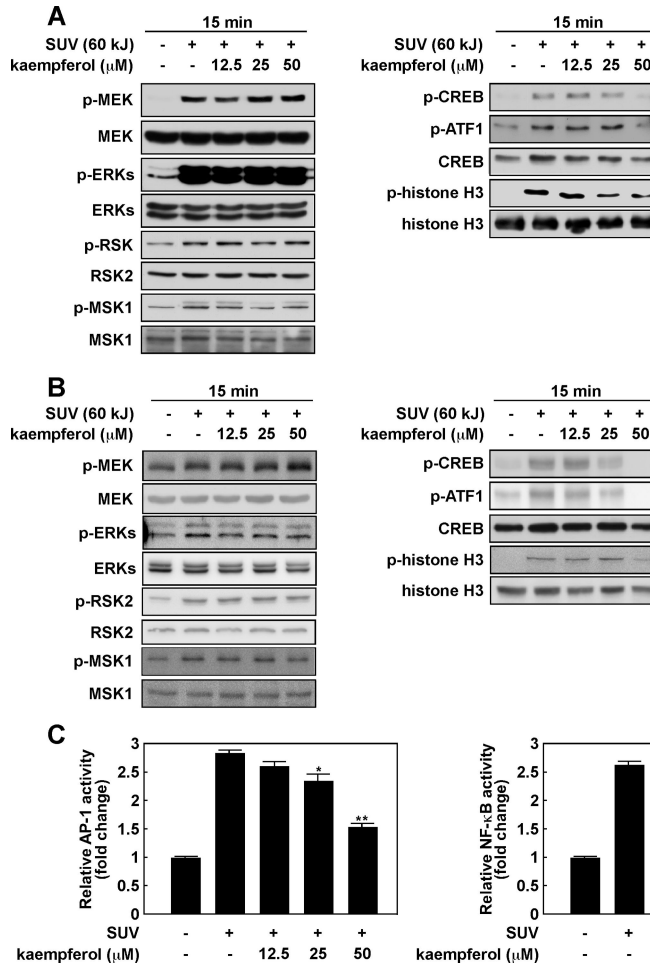


**Figure 4. Kaempferol attenuates UV-induced phosphorylation of CREB and histone H3 and activation of AP-1 and NF- $\kappa$ B in mouse skin cells**

(A) The effect of kaempferol on UV-induced phosphorylation in MAP kinase signaling cascades in JB6 P+ mouse skin epidermal cells (A) and primary mouse keratinocytes (B). The cells were cultured, pretreated with kaempferol for 30 min and then treated with UV (60 kJ/m<sup>2</sup>) and harvested 15 min after UV treatment. Proteins were extracted and protein levels were analyzed by Western blotting with specific antibodies as indicated. (C) Kaempferol inhibits AP-1 and NF- $\kappa$ B activity induced by UV induction. For the luciferase assay, JB6 P+ cells stably transfected with an AP-1 or NF- $\kappa$ B luciferase reporter plasmid were cultured. Cells were incubated in serum-free medium for 24 h, and then treated with kaempferol (0-50  $\mu$ M), or its vehicle, DMSO (negative control), in serum-free medium for 2 h. Cells were then exposed to UV (60 kJ/m<sup>2</sup>) and harvested 3 h later. Luciferase activity was measured and AP-1 or NF- $\kappa$ B activity is expressed relative to control cells without UV treatment. Data are shown as mean values  $\pm$  S.D. obtained from triplicate experiments. Significant differences were evaluated using one-way ANOVA and the asterisks indicate a significant effect (\*,  $p < 0.05$ ; \*\*,  $p < 0.01$ ).



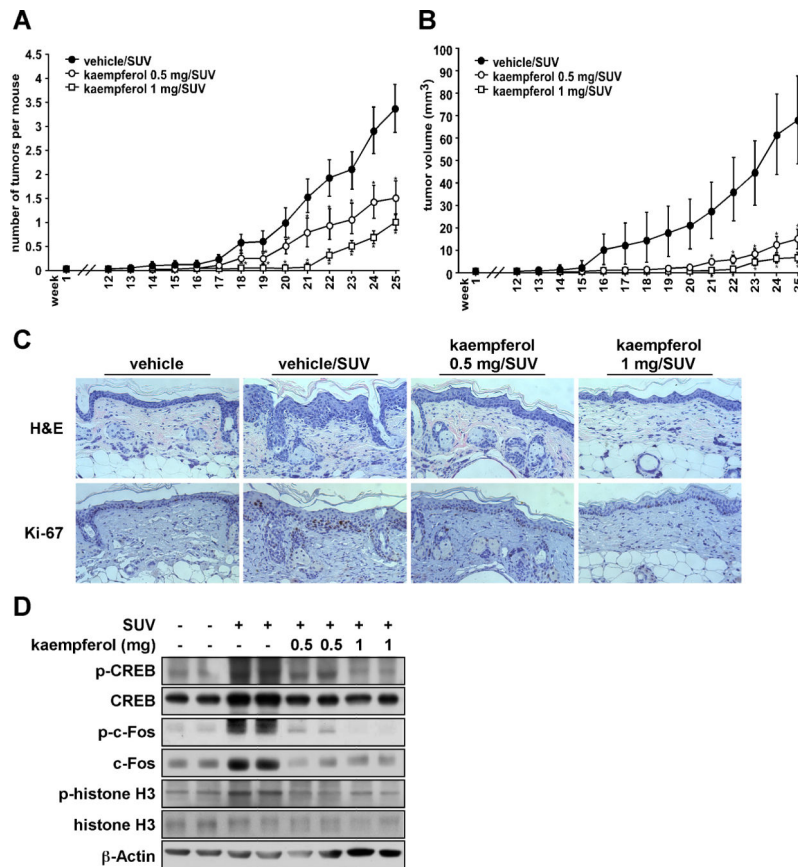


**Figure 5. Kaempferol significantly suppresses SUV-induced skin carcinogenesis in a mouse skin tumorigenesis model**

SKH-1 hairless mice were treated as described in Materials and Methods. The mice in the vehicle group ( $n = 12$ ) received topical treatment with acetone or 1.0 mg kaempferol only. In the vehicle/SUV-treated group ( $n = 24$ ), the mice were treated with acetone before SUV exposure. The mice in the 0.5 mg/SUV or 1.0 mg/SUV groups ( $n = 24$  each) received treatment with kaempferol (0.5 or 1.0 mg, respectively) before SUV exposure. The frequency of irradiation was set at 3 times a week for 10 weeks. The respective doses of acetone or kaempferol were applied topically to the dorsal area. Tumor incidence and multiplicity were recorded weekly until the end of the experiment at week 25. (A) Kaempferol suppresses SUV-induced average tumor number and (B) volume. Tumor volume was calculated according to the following formula: tumor volume ( $\text{mm}^3$ ) = length X width X height X 0.52. A and B, data are represented as means  $\pm$  S.E. and differences were determined by one-way ANOVA. The asterisk (\*) indicates a significant decrease compared to the vehicle/SUV-treated group ( $p < 0.01$ ). (C) Kaempferol inhibits chronic inflammation and proliferation induced by SUV in mouse skin epidermal tissue. Dorsal trunk skin samples were harvested and stained with H&E (upper panels) and with an antibody to detect Ki-67 (lower panels). Representative staining shows the thickness and Ki-67 staining of the epidermis from each of the groups. Stained cells were counted from 5 separate areas on each slide and an average of 3 samples was examined per group. (D) Kaempferol inhibits SUV-

induced phosphorylation of c-Fos, CREB and histone H3 in mouse skin. The expression levels of phosphorylated and total proteins were analyzed by Western blot.